JACS
JOURNAL OF THE AMERICAN CHEMICAL SOCIETY
Communication
pubs.acs.org/JACS

Synthesis and Reactivity of a Transient, Terminal Nitrido Complex of Rhodium

Markus G. Scheibel,[†] Yanlin Wu,[†,¶] A. Claudia Stückl,[†] Lennard Krause,[†] Elena Carl,[†] Dietmar Stalke,[†] Bas de Bruin,*[,‡] and Sven Schneider*[,†]

[†]Institut für Anorganische Chemie, Georg-August-Universität, Tammannstraße 4, 37077 Göttingen, Germany

[‡]Homogeneous and Supramolecular Catalysis group, van't Hoff Institute for Molecular Sciences (HIMS), University of Amsterdam, 1090 GD Amsterdam, The Netherlands

Supporting Information

ABSTRACT: Irradiation of rhodium(II) azido complex $[Rh(N_3)\{N(CHCHP^tBu_2)_2\}]$ allowed for the spectroscopic characterization of the first reported rhodium complex with a terminal nitrido ligand. DFT computations reveal that the unpaired electron of rhodium(IV) nitride complex $[Rh(N)\{N(CHCHP^tBu_2)_2\}]$ is located in an antibonding Rh−N π^* bond involving the nitrido moiety, thus resulting in predominant N-radical character, in turn providing a rationale for its transient nature and observed nitride coupling to dinitrogen.

Transition metal (TM) complexes with oxo and nitrido ligands play pivotal roles in important biological and synthetic transformations, such as C−H functionalization, O_2 reduction, or nitrogen fixation. Both ligands can donate up to six electrons, hence requiring three vacant metal d-orbitals with suitable symmetry for bonding. The electronic structure of octahedral TM oxo complexes was first described by Ballhausen and Gray, providing criteria to estimate stability and reactivity.[1] Oxo complexes with tetragonal symmetry and $d^{n>2}$ valence electrons exhibit populated M−O π^*-orbitals, hence, their intrinsic instability and scarcity beyond group 8 ('oxo wall').[2] Accordingly, exceptions exhibit lower coordination numbers stabilized by bulky ligand environments.[3]

Likewise, beyond the few electron-rich (d^4) group 8 nitrides,[4−6] only two stable, terminal nitrido complexes (both Ir) were reported (Chart 1, **1** and **2**).[7,8] Also, transient nitride **3**

Chart 1. Nitrido Complexes of Iridium (1−3) and Iron(V) Nitride 4

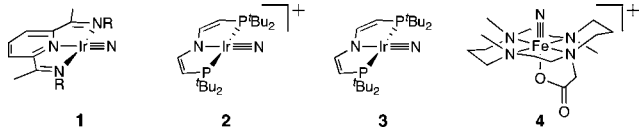

could be characterized spectroscopically. **3** rapidly decomposes by nitride coupling to give N_2, which was attributed to the partial *N*-centered radical character.[8,9] Recent efforts to obtain Co[10] and Rh[11] nitrides resulted in the isolation of C−H insertion products, as also found for the thermolysis of **1** and for some transient molecular nitrides of Fe,[12] U,[13] and Ru.[14] In this contribution we report the first spectroscopic characterization of a terminal rhodium nitrido complex.

The reaction of *Wilkinson's complex* $[Rh(Cl)(PPh_3)_3]$ with $HN(CH_2CH_2P^tBu_2)_2$ and *in situ* oxidation with benzoquinone affords rhodium(II) pincer complex $[RhCl\{N(CHCHP^tBu_2)_2\}]$ (**5**) as a green solid in around 50% isolated yield, similar to the corresponding iridium(II) complex (Scheme 1).[15] The mechanism for the formation of **5** was

Scheme 1. Synthesis and Reactivity of Rhodium Nitrido Complex 7

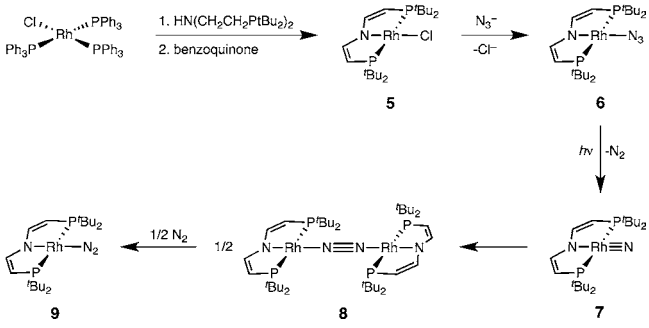

not examined. However, without an oxidizing agent the rhodium(I) complex $[Rh(PPh_3)\{HN(CH_2CH_2P^tBu_2)_2\}]Cl$ was isolated and crystallographically characterized (Supporting Information [SI]), probably representing an intermediate prior to backbone dehydrogenation. Salt metathesis of **5** with a mixture of $[N(PPh_3)_2]N_3/NaN_3$ (1:9) in acetone gives the azido complex $[Rh(N_3)\{N(CHCHP^tBu_2)_2\}]$ (**6**) in almost quantitative yield.

Two (**5**) and three (**6**) paramagnetically broadened and shifted signals in the ^{1}H NMR spectra, respectively, indicate C_{2v} symmetry on the NMR time scale. The missing backbone proton signal of **5** is assumed to be superimposed with the broad and intense signal of the *t*Bu group, as indicated by the peak integral. Note, that these two signals are close in the case of complex **6** as well ($\Delta\delta$ = 3.0 ppm). The magnetic moment of **5** (1.7 μ_B, Evans' method) is in agreement with an S = 1/2 ground state. The large anisotropy of the **g**-tensors (**5**: g_{11} = 3.25, g_{22} = 1.82, g_{33} = 1.68; **6**: g_{11} = 2.92, g_{22} = 1.96, g_{33} = 1.85)

Received: September 23, 2013
Published: November 15, 2013

   dx.doi.org/10.1021/ja409764j | J. Am. Chem. Soc. 2013, 135, 17719−17722

in the rhombic EPR spectra of **5** (SI, Figure S1) and **6** (Figure 1) indicate the presence of metal-centered (Rh^{II}) radical

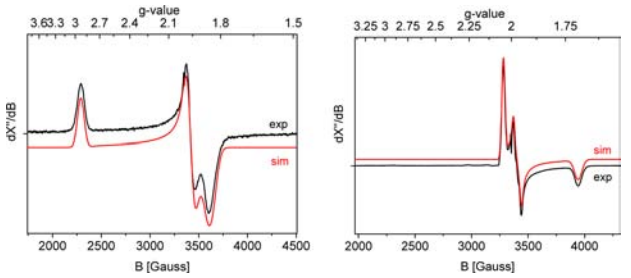

Figure 1. Experimental and simulated EPR spectra in frozen toluene (T = 20 K, F_{req} = 9.380845 GHz, modulation amplitude 4 G, microwave power 0.2 mW). *Left*: Rhodium azido complex **6**. *Right*: Rhodium nitrido species **7** obtained by irradiation of **6** with UV light in the glass.

complexes. Rhodium hyperfine coupling is not resolved. The azide stretching vibration of **6** was assigned to a strong peak at 2040 cm^{-1} in the IR spectrum. DFT electronic structure (b3lyp/def2-TZVP) and EPR (BP86/ZORA/TZP) property calculations are in good agreement with the spectroscopic results (**5**: g_{11} = 3.13, g_{22} = 1.81, g_{33} = 1.52; **6**: g_{11} = 2.79, g_{22} = 1.94, g_{33} = 1.79) and corroborate the assignments as rare examples of square-planar rhodium(II) complexes (Mulliken spin density on Rh: 81% (**5**), 74% (**6**)).[16] The molecular structure of **5** was also determined by single-crystal X-ray diffraction (Figure 2), confirming the square-planar coordination geometry around the metal.

Irradiation of **6** in frozen toluene at 20 K led to the gradual disappearance of its EPR signal and clean formation of exclusively one new signal (Scheme 1, Figure 1). All components of the rhombic **g**-tensor (g_{11} = 2.04, g_{22} = 1.93, g_{33} = 1.70) are close to or well below the value for the free electron (g_e = 2.002). This new signal was assigned to rhodium(IV) nitride [Rh(N){N(CHCHP*t*Bu_2)$_2$}] (**7**). The EPR spectrum of **7** is similar to that of iridium(IV) nitrido complex **3** (g_{11} = 1.89, g_{22} = 1.63, g_{33} = 1.32), for which the unusual **g**-tensor was rationalized on the basis of extensive mixing via spin−orbit coupling of the nearly degenerate SOMO and LUMO, which exhibit strong Ir≡N π^*-MO character.[8] The smaller orbital contributions to the **g**-tensor of **7**, in comparison to that of **3**, are in agreement with the smaller spin−orbit coupling (SOC) constant of rhodium.[17] In contrast to **3**, hyperfine interactions (HFI) are resolved along one direction of the HFI tensor. The clearly resolved ^{14}N hyperfine coupling (A_{22} = +65 MHz) is close to the value found for **3** by Davies ENDOR spectroscopy (A_{22} = +64 MHz),[8] further indicating similar electronic structures of **3** and **7**. Spectral simulations and line shape analyses point to a smaller ^{103}Rh hyperfine coupling of ∼25 MHz along g_{22}.

The formation of a nitrido complex is further supported by vibrational spectroscopy. Short irradiation of a KBr pellet of **6** causes the appearance of a weak band at 874 cm^{-1} in the IR spectrum (see SI, Figure S4), which was assigned to the Rh≡N stretching vibration of **7**. The band disappears on extended irradiation. Upon use of partially ^{15}N-azide labeled **6** a second band at 848 cm^{-1} was also observed (Figure S5, SI) which is in excellent agreement with the harmonic oscillator approximation for the $^{14}N/^{15}N$-**7** isotopologues (26 cm^{-1}). These values are also in excellent agreement with the DFT computed stretching

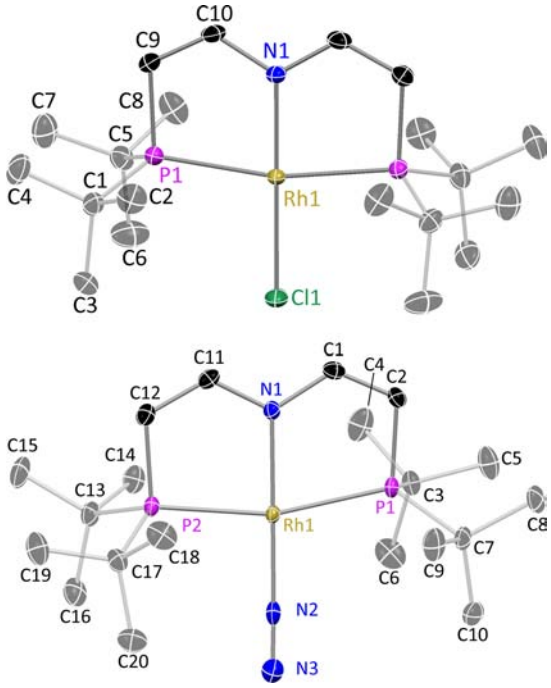

Figure 2. DIAMOND plots of the molecular structures of **5** (top) and **9** (bottom) from single-X-ray diffraction (ellipsoids set at 50% probability, hydrogen atoms are omitted for clarity). Selected bond lengths [Å] and angles [deg]: **5**: Rh1−Cl1 2.3344(7), Rh1−N1 1.9667(14), Rh1−P1 2.3249(7), C9−C10 1.3499(16); N1−Rh1−Cl1 180, P1−Rh1−P1′ 166.573(16). **9**: Rh1−N1 2.025(3), Rh1−N2 1.911(3), Rh1−P1 2.3246(10), Rh1−P2 2.3165(10), N2−N3 1.091(4), C1−C2 1.351(5), C11−C12 1.354(5); N1−Rh1−N2 177.93(11), P1−Rh1−P2 164.12(3).

frequencies for **7** (^{14}N: 871 cm^{-1}; ^{15}N: 842 cm^{-1}) upon applying the same scaling factor as was used for **2** and **3**. Notably, the M≡N stretching vibration of **7** is slightly lower than that in the analogous iridium complex **3** (901 cm^{-1}). Hence, the ratio of the harmonic oscillator force constants ($f_{Rh}/f_{Ir} = \nu_{Rh}^2\mu_{Rh}/\nu_{Ir}^2\mu_{Ir}$ = 0.88) indicates weaker Rh≡N than Ir≡N bonding. In agreement, DFT calculations reveal a weaker M≡N Mayer bond order for rhodium compared to that for iridium (Rh: 1.972; Ir: 2.290), and also formation of the nitrido species from its azido precursor is calculated to be less exergonic ($\Delta G°_{298K}$ Rh: −4.7 kcal mol^{-1}; Ir: −14.3 kcal mol^{-1}) and has a higher kinetic barrier ($\Delta G^{‡}_{298K}$ Rh: +33.4 kcal mol^{-1}; Ir: +27.8 kcal mol^{-1}).

The EPR spectroscopic assignments were also substantiated computationally. According to DFT, the electronic structure of **7** is analogous to that of **3**. The SOMO (MO 111α, Figures 3 and S11, SI) represents an antibonding interaction between the metal (d_{xz}) and the nitrido ligand (p_z). As for complex **3**, the

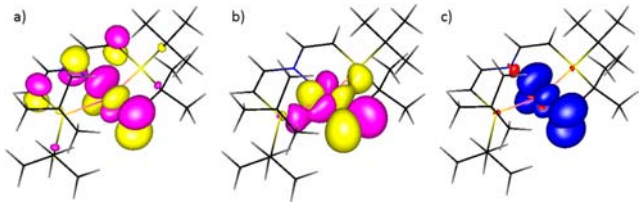

Figure 3. (a) SOMO (MO 111α), (b) LUMO (MO 112α), and (c) spin density plots of **7**.

dx.doi.org/10.1021/ja409764j | J. Am. Chem. Soc. 2013, 135, 17719−17722

other predominantly M−N π^* antibonding orbital is close in energy (LUMO: MO 112α) and exhibits the appropriate (rotational) symmetry for efficient SOMO/LUMO excited state admixture of orbital angular momentum into the ground state via SOC. The spin density distribution of **7** has the same shape as the SOMO (Figure 3), indicating minor effects of spin polarization on the distribution. Hence, the unpaired electron is mainly situated in a π^* Rh−N orbital. As a consequence of the high degree of covalency within the Rh≡N π-bonding the spin density is strongly delocalized over this moiety, exhibiting a preference for the N (∼64%) over the Rh (∼37%) atom according to Mulliken spin-densities (b3-lyp, def2-TZVP). Hence, the nitridyl-radical character of Rh complex **7** is even higher (and better defined due to smaller SOC contributions) than for Ir complex **3** (∼50% spin density at N).[8] The experimental **g**-tensor (g_{11} = 2.04, g_{22} = 1.97, g_{33} = 1.70) and the resolved ^{14}N HFI value along g_{22} (A_{22} = 65 MHz) of **7** are well reproduced by DFT property computations (g_{11} = 2.02, g_{22} = 1.93, g_{33} = 1.62; A^{N}_{22} = 52 MHz; see also SI), thus giving confidence in the calculated electronic structure.

Upon thawing a frozen solution of **7**, the EPR signature immediately disappears. Two diamagnetic molecules are formed after photolysis in frozen solution or in the liquid phase at −60 °C. Their ratio is subject to the reaction conditions: Irradiation in solution under an atmosphere of dinitrogen produces the rhodium(I) complex [Rh(N_2){N-(CHCHP*t*Bu$_2$)$_2$}] (**9**), selectively, which was fully characterized including single-crystal X-ray diffraction (Figure 2). The IR spectrum of **9** exhibits an intense band at 2120 cm^{-1} that can be assigned to the N−N stretching vibration. NMR characterization (^{31}P: 78 ppm) is in agreement with C_{2v} symmetry in solution. However, irradiation of **6** in solution under vacuum results in partial formation of **9** (34%). The isolation of the main product (66%) was unsuccessful, owing to very similar solubility, but NMR (^{31}P: 75 ppm) and electrospray mass spectrometry (ESI-MS) characterization are in agreement with the assignment to bridging dinitrogen complex [(μ_2-μ^2-N_2){NRh(CHCHP*t*Bu$_2$)$_2$}$_2$] (**8**). The use of partially ^{15}N-labeled **6** enabled the detection of the N_2 ligand by ^{15}N NMR spectroscopy (δ = −76 ppm) and of all three possible isotopomers (^{15}N^{15}N-**8**, ^{15}N^{14}N-**8**, and ^{14}N^{14}N-**8**) by ESI-MS, confirming that the azide group is the source for N_2 formation (see SI, Figure S7).

These results are in agreement with coupling of the transient nitride **7** to a bridging N_2 complex (**8**) which dissociates to the terminal N_2 complex **9** in the presence of excess N_2, e.g. from azide splitting (Scheme 1). In contrast to the previously reported iridium(IV) nitride **3**,[8] the corresponding rhodium-(IV) nitride **7** is too reactive to be detected in the liquid phase. It is tempting to attribute the lower thermal stability of **7** to the enhanced *N*-radical character.[9] In agreement with these observations, the DFT calculated barrier for N−N coupling is lower for rhodium ($\Delta G^{\ddagger}_{298K}$ = +11.9 kcal mol^{-1}) than for iridium ($\Delta G^{\ddagger}_{298K}$ = +13.7 kcal mol^{-1}).

Interestingly, irradiation of **6** in the presence of 10 equiv of 1,4-cyclohexadiene (BDE_{C-H} = +76 kcal mol^{-1})[18] gave the same product (**8**) as without the hydrogen donor reagent (DFT estimated BDE_{N-H} of [(L^{Me})Rh(NH)]: +78.7 kcal mol^{-1}). In good agreement, DFT calculations reveal a substantially higher kinetic barrier for HAT from 1,4-cyclohexadiene to [(L^{Me})Rh(N)] ($\Delta G^{\ddagger}_{298K}$ = +21.9 kcal mol^{-1}) as compared to the barrier for N−N coupling of two nitridyl radical species ($\Delta G^{\ddagger}_{298K}$ = +11.9 kcal mol^{-1}) to form [(L^{Me})Rh(N_2)Rh(L^{Me})]. See SI for a more detailed description of all DFT calculated pathways, including computed changes in bond orders and bond lengths.

In conclusion, we report the first spectroscopic characterization of a terminal rhodium nitrido complex. Analysis of the EPR data of **7** with the aid of DFT property calculations reveals an intriguing electronic structure. The unpaired electron of **7** is mainly localized in a nearly covalent Rh−N π^* bond, leading to substantial spin density at the nitrido/nitridyl moiety (∼60%). Hence, the 'Rh^{IV}-nitrido' species is best described as being in between the resonance structures [(PNP)Rh^{IV}•(N^{3-})] and [(PNP)Rh^{III}(•N^{2-})], with a slightly dominating 'nitridyl radical' contribution. As was shown for analogous Ir nitride **3**, the transient rhodium nitride **7** readily reacts via radical-type N−N coupling to the corresponding dimeric rhodium(I) N_2 complex **8**. This mechanistic pathway might similarly apply to d^3 nitrides, such as iron(V) nitride **4** (Chart 1),[19−21] pointing toward a fundamental electronic structure−reactivity relationship for isolobal square-planar {M−N}^{5} and octahedral {M−N}^{3} complexes.[22] Given the highly transient nature of these compounds, the selectivity of decay by N−N coupling is remarkable even in the presence of weak C−H bonds.

■ ASSOCIATED CONTENT

Ⓢ Supporting Information

Full preparative, analytical, crystallographic, and computational details in pdf format. This material is free of charge via the Internet at http://pubs.acs.org.

■ AUTHOR INFORMATION

Corresponding Authors

sven.schneider@chemie.uni-goettingen.de
b.debruin@uva.nl

Present Address

¶Department Chemie and Pharmazie, Friedrich-Alexander-Universität Erlangen-Nürnberg, Egerlandstraße 1, 91058 Erlangen, Germany.

Notes

The authors declare no competing financial interest.

■ ACKNOWLEDGMENTS

S.S. is grateful to the Deutsche Forschungsgemeinschaft for funding (*Emmy Noether Programm* SCHN950/2). B.d.B. gratefully acknowledges financial support by NWO−CW (VICI grant 016.122.613, BdB). D.S. thanks the Danish National Science Foundation (DNSF93) funded *Center of Materials Crystallography* (CMC) for partial support.

■ REFERENCES

(1) Ballhausen, C. J.; Gray, H. B. *Inorg. Chem.* **1962**, *1*, 111.
(2) Winkler, J. R.; Gray, H. B. *Struct. Bonding (Berlin)* **2012**, *142*, 17.
(3) (a) Hay-Motherwell, R. S.; Wilkinson, G.; Hussein-Bates, B.; Hursthouse, M. B. *Polyhedron* **1993**, *12*, 2009. (b) Poverenov, E.; Efremenko, I.; Frenkel, A. I.; Ben-David, Y.; Shimon, L. J. W.; Leitus, G.; Konstantinovski, L.; Martin, J. M. L.; Milstein, D. *Nature* **2008**, *455*, 1093.
(4) (a) Berry, J. F. *Comments Inorg. Chem.* **2009**, *30*, 28. (b) Saouma, C. T.; Peters, J. C. *Coord. Chem. Rev.* **2011**, *255*, 920. (c) Hohenberger, J.; Ray, K.; Meyer, K. *Nat. Commun.* **2012**, *3*, 720.
(5) (a) Betley, T. A.; Peters, J. C. *J. Am. Chem. Soc.* **2004**, *126*, 6252. (b) Vogel, C.; Heinemann, F. W.; Sutter, J.; Anthon, C.; Meyer, K. *Angew. Chem., Int. Ed.* **2008**, *47*, 2681. (c) Scepaniak, J. J.; Fulton, M. D.; Bontchev, R. P.; Duesler, E. N.; Kirk, M. L.; Smith, J. M. *J. Am.*

Chem. Soc. **2008**, *130*, 10515. (d) Scepaniak, J. J.; Young, J. A.; Bontchev, R. P.; Smith, J. M. *Angew. Chem., Int. Ed.* **2009**, *48*, 3158.
(6) (a) Walstrom, A.; Pink, M.; Yang, X.; Tomaszewski, J.; Baik, M.-H.; Caulton, K. G. *J. Am. Chem. Soc.* **2005**, *127*, 5330. (b) Askevold, B.; Nieto, J. T.; Tussupbayev, S.; Diefenbach, M.; Herdtweck, E.; Holthausen, M. C.; Schneider, S. *Nat. Chem.* **2011**, *3*, 532.
(7) (a) Schöffel, J.; Rogachev, A. Y.; DeBeer George, S.; Burger, P. *Angew. Chem., Int. Ed.* **2009**, *48*, 4734. (b) Sieh, D.; Schöffel, J.; Burger, P. *Dalton Trans.* **2011**, *40*, 9512.
(8) Scheibel, M. G.; Askevold, B.; Heinemann, F. W.; Reijerse, E. J.; de Bruin, B.; Schneider, S. *Nature Chem.* **2012**, *4*, 552.
(9) Olivos Suarez, A. I.; Lyaskovskyy, V.; Reek, J. N. H.; van der Vlugt, J. I.; de Bruin, B. *Angew. Chem. Int. Ed* **2013**, DOI: 10.1002/anie.201301487.
(10) Atienza, C. C. H.; Bowman, A. C.; Lobkovsky, E.; Chirik, P. J. *J. Am. Chem. Soc.* **2010**, *132*, 16343.
(11) Schöffel, J.; Susnjar, N.; Nückel, S.; Sieh, D.; Burger, P. *Eur. J. Inorg. Chem.* **2010**, 4911.
(12) Schlangen, M.; Neugebauer, J.; Reiher, M.; Schröder, D.; Lopez, J. P.; Haryono, M.; Heinemann, F. W.; Grohmann, A.; Schwarz, H. *J. Am. Chem. Soc.* **2008**, *130*, 4285.
(13) Thomson, R. K.; Cantat, T.; Scott, B. L.; Morris, D. E.; Batista, E. R.; Kiplinger, J. L. *Nat. Chem.* **2010**, *2*, 723.
(14) Long, A. K. M.; Yu, R. P.; Timmer, G. H.; Berry, J. F. *J. Am. Chem. Soc.* **2010**, *132*, 12228.
(15) Meiners, J.; Scheibel, M. G.; Lemée-Cailleau, M.-H.; Mason, S. A.; Boeddinghaus, M. B.; Fässler, T. F.; Herdtweck, E.; Khusniyarov, M. M.; Schneider, S. *Angew. Chem., Int. Ed.* **2011**, *50*, 8184.
(16) (a) Pandey, K. K. *Coord. Chem. Rev.* **1992**, *121*, 1. (b) DeWitt, D. G. *Coord. Chem. Rev.* **1996**, *147*, 209. (c) Poli, R. *Chem. Rev.* **1996**, *96*, 2135. (d) de Bruin, B.; Hetterscheid, D. G. H.; Koekkoek, A. J. J.; Grützmacher, H. *Prog. Inorg. Chem.* **2007**, *55*, 247. (d) Feller, M.; Ben-Ari, E.; Gupta, T.; Shimon, L. J. W.; Leitus, G.; Diskin-Posner, Y.; Weiner, L.; Milstein, D. *Inorg. Chem.* **2007**, *46*, 10479.
(17) Goodman, B. A.; Raynor, J. B. *Adv. Inorg. Chem. Radiochem.* **1970**, *13*, 136.
(18) Warren, J. J.; Tronic, T. A.; Mayer, J. M. *Chem. Rev.* **2010**, *110*, 6961.
(19) Kane-Maguire, L. A. P.; Sheridan, P. S.; Basolo, F.; Pearson, R. G. *J. Am. Chem. Soc.* **1970**, *92*, 5865.
(20) (a) Buhr, J. D.; Taube, H. *Inorg. Chem.* **1979**, *18*, 2208. (b) Ware, D. C.; Taube, H. *Inorg. Chem.* **1991**, *30*, 4605. (c) Lam, H. W.; Che, C.; Wong, K. Y. *J. Chem. Soc., Dalton Trans.* **1992**, 1411. (d) Demadis, K. D.; El-Samanody, E. S.; Coia, G. M.; Meyer, T. J. *J. Am. Chem. Soc.* **1999**, *121*, 535.
(21) Aliaga-Alcalde, M.; DeBeer George, S.; Mienert, B.; Bill, E.; Wieghardt, K.; Neese, F. *Angew. Chem., Int. Ed.* **2005**, *44*, 2908.
(22) Bendix, J.; Meyer, K.; Weyhermüller, T.; Bill, E.; Metzler-Nolte, N.; Wieghardt, K. *Inorg. Chem.* **1998**, *37*, 1767.